General Disclaimer

One or more of the Following Statements may affect this Document

- This document has been reproduced from the best copy furnished by the organizational source. It is being released in the interest of making available as much information as possible.

- This document may contain data, which exceeds the sheet parameters. It was furnished in this condition by the organizational source and is the best copy available.

- This document may contain tone-on-tone or color graphs, charts and/or pictures, which have been reproduced in black and white.

- This document is paginated as submitted by the original source.

- Portions of this document are not fully legible due to the historical nature of some of the material. However, it is the best reproduction available from the original submission.

NASA Technical Memorandum 83576

Analytical Study of Blowing Boundary-Layer Control for Subsonic V/STOL Inlets

Danny P. Hwang
Lewis Research Center
Cleveland, Ohio

Prepared for the
Seventh Annual Energy-Sources Technology Conference and Exhibition
sponsored by the American Society of Mechanical Engineers
New Orleans, Louisiana, February 12–16, 1984

NASA

E-1963

ANALYTICAL STUDY OF BLOWING BOUNDARY LAYER CONTROL FOR SUBSONIC V/STOL INLETS

Danny P. Hwang

National Aeronautics and Space Administration
Lewis Research Center
Cleveland, Ohio 44135

ABSTRACT

The analytical methods used to study blowing boundary-layer control (BLC) for subsonic V/STOL inlets at the NASA Lewis Research Center are briefly described. The methods are then shown to give good agreement with experimental results, both with and without blowing BLC. Finally, because of this good agreement, the methods have been used to determine analytically the optimum (minimum blowing power required) location and height for a blowing slot within a subsonic V/STOL inlet. Results of this analytical study are presented.

NOMENCLATURE

a	major axis of internal lip of inlet (fig. 3)
b	minor axis of internal lip of inlet (fig. 3)
CR	contraction ratio, $(D_{hl}/D_t)^2$
C_p	constant-pressure specific heat
C_w	relative blowing-power coefficient
D	diameter
H	blowing slot height
L	axial length (fig. 3)
M	Mach number
$\dot{m}$	mass flow rate, kg/sec
P	total pressure
p	static pressure
S	surface distance from stagnation point
T	total temperature
V	velocity
$\dot{W}$	ideal blowing power
X	axial distance from highlight
Y	vertical distance from inlet surface
α	angle of attack, deg
γ	ratio of specific heat (γ = 1.1 for air)
δ	boundary-layer thickness
θ_m	diffuser maximum local wall angle (fig. 3), deg

Subscripts:

B	blowing jet
c	centerbody
d	diffuser
de	diffuser exit
e	boundary-layer edge
hl	highlight
i	inlet
j	blowing jet
m	maximum
ref	reference
t	throat
0	free stream

INTRODUCTION

In recent years, many different propulsion-system concepts have been proposed for subsonic V/STOL aircraft. One of the concepts is a tilt-nacelle propulsion system where the entire engine rotates through 90° to provide vertical thrust for takeoff and landing, as shown in figure 1. The inlet of this type of nacelle can be subjected to an angle of attack as high as 120°. At these severe flow conditions, special design techniques are required to maintain attached internal flow for high inlet efficiency (high total-pressure recovery and low distortion). Blowing boundary-layer control (BLC) is one of these techniques. Because the blowing power is readily available from the engine, this technique seems to be very attractive.

The application of blowing BLC to maintain attached internal flow in a subsonic V/STOL inlet is similar to that for airfoils (refs. 1 to 3). In both

cases, the weak boundary layer is energized by tangential injection of a high-velocity jet to avoid flow separation. Blowing BLC for high-angle-of-attack inlets has been investigated experimentally, and the results are reported in reference 2. This reference also includes some analytical results for blowing BLC from a series of subsonic-inlet computer programs that have been developed at the NASA Lewis Research Center. These programs are described, in detail, in references 4 and 5. Results of experimental studies (refs. 6 to 10) have been used to substantiate the analytical methods and are summarized in reference 11.

In this paper, the methods used for analyzing subsonic inlets with blowing BLC (and also without BLC) are described and compared with experimental results. The analytical and experimental results are shown to be in good agreement. Finally, the analytical methods are used to establish the optimum location and geometry of the BLC blowing slot on a subsonic V/STOL inlet. Optimum, in this case, refers to the minimum power required to provide the pressurized airflow for the BLC system.

BASIC METHOD OF ANALYSIS

The series of computer programs used at the NASA Lewis Research Center for subsonic axisymmetric inlet analysis is depicted in figure 2. A geometry package creates the discrete control points for each geometric configuration. Then, an incompressible potential flow program (refs. 12 and 13) is used to calculate the basic solutions to the problem. The basic solutions consist of a static solution (i.e., $V_0 = 0$), a uniform axial flow solution, and a 90°-angle-of-attack solution. These basic solutions are combined into one that satisfies the specified inlet operating conditions of free-stream velocity, angle of attack, and inlet mass flow (ref. 4). Next, the incompressible flow solution is corrected for compressibility effects by the method of Lieblein and Stockman (ref. 14). The compressible potential flow solution is then used as an input to the Herring boundary-layer program (ref. 5) which calculates the laminar, transition, and turbulent boundary-layer characteristics. The boundary-layer program also permits the inclusion of a blowing jet for boundary-layer control. Two iteration loops have been built into the analysis method and are illustrated in figure 2. The first adds the displacement thickness to the geometry to improve the accuracy of the potential flow and boundary-layer calculations. The second incorporates an automatic blowing slot height and blowing jet velocity iteration loop at a fixed blowing slot location in one uninterrupted computer run.

For a fixed blowing jet location, this second iteration loop selects a value of slot height and then calculates the minimum blowing jet velocity required to just attach the boundary layer. The loop then continues with the slot height being changed and the jet velocity variation repeated. The net result of the loop is the minimum blowing jet velocity required to maintain an attached boundary layer for a range of slot heights at a given slot location. The whole process can then be repeated for a range of locations.

In order to help judge which combination of slot location, height, and blowing jet velocity would be most desirable, the blowing relative power coefficient, C_w, is calculated for each case. This coefficient is derived from the following equations:

$$\dot{W} = \dot{m}_j C_p T_0 \left[\left(\frac{P_B}{P_0} \right)^{\frac{\gamma-1}{\gamma}} - 1 \right] \tag{1}$$

$$\dot{W}_{ref} = \dot{m}_{ref} C_p T_0 (10)^{-4} \tag{2}$$

$$C_w = \dot{W}/\dot{W}_{ref} \tag{3}$$

$$C_w = \frac{\dot{m}_j}{\dot{m}_{ref}} \left[\left(\frac{P_B}{P_0} \right)^{\frac{\gamma-1}{\gamma}} - 1 \right] (10)^4 \tag{4}$$

where $\dot{W}$ is the ideal blowing power required to raise the total pressure of the blowing air flow from free-stream total pressure, P_0, to the blowing total pressure, P_B; and $\dot{W}_{ref}$ is a reference power used to nondimensionalize $\dot{W}$. One method for selecting an optimum blowing slot location and height would be to minimize C_w. Results of such an optimization will be discussed in a later section of this paper.

COMPARISON OF ANALYTICAL AND EXPERIMENTAL RESULTS

An experimental research model of the inlet has been tested in the Lewis 9x15-Foot Low Speed Wind Tunnel to evaluate the effectiveness of blowing BLC with subsonic V/STOL inlets. Test results from these experiments (ref. 2) have been used to verify the just described analytical methods for both non-blowing and blowing BLC cases. The inlet geometry used for the analytical study is shown in figure 3, and some of the more significant inlet design parameters are listed on the figure.

The results of the axisymmetric potential flow calculation with compressibility correction along with experimental results are shown in figure 4. Figure 4(a) shows the internal static pressure distribution on the inlet windward surface at a free-stream Mach number of 0.184, an angle of attack of 39.6°, and a mass flow rate of 17.96 kg/sec. The agreement with experiment is excellent. As shown in figure 4(b), however, when the angle of attack is increased to 44.5° and mass flow rate is increased to 27.69 kg/sec, the agreement with experiment is not quite as good. The peak Mach number for this case is 1.5, and a shock/boundary-layer interaction would be expected to occur at these conditions. The current computer programs cannot handle this type of interaction, and this fact may account in part for the difference between experiment and analysis shown in the figure. This figure also illustrates the improvement in the analytical results when the displacement thickness correction is made.

Figure 5 shows another comparison of the analytical predictions and the experimental results in terms of the internal flow separation boundaries for the inlet with and without blowing BLC. The figure shows the inlet angle of attack at which the internal flow separates for a given value of the ratio of inlet throat velocity to free-stream velocity - a ratio that has been shown to correlate inlet flow separation results (ref. 2). Except at the higher angles of attack, the agreement with experiment is quite good. Possible explanations for the discrepancies at the higher angles of attack are given in reference 2.

Figure 6 illustrates the good agreement between theory and experiment for the boundary-layer profiles at two locations within the inlet. The agreement is very good at the downstream location, but not quite as good at the upstream location. At the upstream location, the calculated profile is very sensitive to the assumed profile of the BLC jet coming out of the slot. For these calculations, the slot jet was assumed to

have a flat profile which probably does not match the actual profile in the experiment.

The preceding figures and discussion have established the validity of the analytical methods. Now, these methods are used to determine where the blowing slot should be located on the inlet and what the slot height should be for maintaining attached internal flow with the minimum value of the blowing jet power coefficient, C_w.

APPLICATION OF ANALYTICAL METHOD

By examining the inlet operating requirements as dictated by the aircraft operation during takeoff and landing (ref. 15), a most critical inlet operating point can be selected, which then becomes the inlet design point, as shown in figure 7. If the inlet operates separation-free at the critical operating point, then it will operate separation-free at all other points within the aircraft operating envelope.

In figure 7, typical inlet experimental separation boundaries for inlets having contraction ratios of 1.46 and 1.76 are illustrated. A typical inlet requirement curve (ref. 15) is also shown on the figure. As indicated on the figure, even for the contraction ratio of 1.76, the inlet requirement is not satisfied over the full operating range. An estimated separation boundary for an inlet that would meet the requirements is also shown on the figure. (It has simply been drawn more-or-less parallel to the two actual inlet curves.) The tangent point at which this estimated separation boundary curve and the requirement curve intersect is considered to be the inlet design point. Once again, if the inlet operates separation-free at this point, then it will operate separation-free at all other points within the aircraft operating envelope. For this particular inlet/aircraft, the design point is then at an inlet angle of attack of 70°, at an inlet mass flow rate of 14.9 kg/sec, and a free-stream velocity of 61 m/sec. All calculations in this study were made at this inlet design point and with the inlet geometry discussed previously (fig. 3) having a contraction ratio of 1.46.

Results of the blowing BLC analytical calculations are presented in figures 8 to 10 at the inlet design point. Figure 8(a) shows the effect of blowing slot height on the blowing total pressure ratio required to achieve attached inlet flow at a blowing slot location, S/L_i, of 0.55. As the blowing slot height is reduced, total pressure ratio increases exponentially, while blowing mass flow ratio is decreased linearly, as indicated in figure 8(b). From the previously presented relationship for C_w, it is easy to see that C_w is more sensitive to total pressure ratio changes than blowing mass flow changes. Hence, as expected, figure 8(c) indicates that C_w is decreased monotonically when the blowing slot height is increased. As the slot height is increased further, the blowing jet velocity will approach the boundary-layer edge velocity, the blowing total pressure ratio will approach 1.0, and the value of C_w will approach 0. However, this does not imply that the slot height should be selected to be as large as possible. As the slot height goes up, the adverse effect of a rearward-facing step will take place (ref. 2) and become a problem at operating conditions where blowing BLC is not required. For practical design considerations, the blowing slot height, H/D_{de}, should probably not exceed a value of 0.003. Figure 8(c) also shows some fluctuation of the final converged results about the curve drawn through the results. The reason for this small fluctuation is unknown.

To give a quantitative feel for the time involved in these calculations, for a given blowing slot location and blowing slot height, it usually takes 9 to 10 iterations to reach a converged result for blowing jet velocity required to attach the boundary layer. For the IBM 370-3033, the CPU time required is about 200 sec for each converged result, with a total of 123 boundary-layer calculation points along the surface.

The effects of blowing slot location for a fixed blowing slot height, H/D_{de}, of 0.003 are shown in figure 9. When the blowing slot is moved downstream, the blowing total pressure ratio increases slightly, while the blowing jet mass flow ratio decreases slightly, as shown in figures 9(a) and (b). The combination of both indicates that there should exist a minimum value of blowing power coefficient. As shown in figure 9(c), this is indeed the case, with the minimum occurring at $S/L_i = 0.47$. Any other blowing slot location will cause a higher value of C_w for this particular blowing slot height, H/D_{de}, of 0.003.

Calculations like those illustrated in figures 8 and 9 were performed over a full range of blowing slot locations and heights and are summarized in figure 10. Again, all calculations were done at the inlet design point ($V_0 = 61$ m/sec; $\dot{m} = 14.9$ kg/sec; $\alpha = 70°$). The figure is a plot of blowing slot height versus location of the slot, with solid lines of constant relative blowing power coefficient and dashed lines of constant blowing total pressure ratio. If minimizing the relative blowing power coefficient at any given blowing total pressure ratio is an objective (which it may well be in order to minimize the penalty associated with bleeding the blowing air from the propulsion system), then this figure shows what the optimum slot location and height should be for that blowing total-pressure ratio.

Prior to a discussion of the details of the results, a discussion of some practical constraints is in order. First, as mentioned before, the slot height cannot be made overly large, because the downstream-facing step that occurs when blowing BLC is not being used (say at cruise) may actually induce a flow separation. Secondly, although it may be possible to attach the boundary layer by blowing downstream of the calculated separation point, the method of analysis used in this study does not permit such a calculation. Therefore, the boundary shown on the right side of the figure represents a limitation of the analytical method and indicates a predicted location of the flow separation point without blowing BLC. The third constraint to be considered is also a limitation of the analytical method. For each location, there is a local static pressure on the inlet surface that, when combined with the proper blowing jet total pressure, results in choked flow through the slot. At static-to-total pressures less than this critical value, the aerodynamics of the blowing jet cannot be accurately calculated with the analytical methods used in this study. This constraint is shown as the blowing jet choking limit on the figure.

It should be noted that for the particular inlet design analyzed here at its particular design point, blowing pressure ratios (dashed lines) less than 15 provide the needed blowing jet momentum to attach the inlet boundary layer. This suggests that the blowing BLC air could well be provided by the fan rather than the core compressor on a turbofan engine.

If one assumes that the BLC blowing jet air is available from the engine fan or core compressor at a given total pressure ratio, then by examining the constant blowing total pressure curves (dashed lines) in

figure 10, the following conclusions can be reached:

(1) The selection of a blowing slot height depends on the blowing jet total pressure ratio. A smaller slot height is required for a higher blowing total pressure ratio.

(2) For lower blowing jet total pressure ratios, there exists a blowing jet location at which C_w is a minimum. For this particular inlet, the best blowing jet location is at about $S/L_i = 0.51$, just slightly upstream of the inlet throat.

(3) For higher total pressure ratios, C_w is almost a constant. In order to avoid exceeding either the blowing jet choking limit or the separation limit, the best location for the blowing jet would again appear to be about halfway between the two limits, that is, at $S/L_i = 0.51$.

(4) As the blowing slot location approaches the inlet highlight (leading edge), the slot may choke. This, in turn, leads to aerodynamic flow characteristics within the blowing jet flow field and the boundary layer that cannot be adequately analyzed by the methods used for this study.

CONCLUDING REMARKS

Analytical investigations were conducted to evaluate the effectiveness of blowing BLC for subsonic V/STOL inlets. The results of the investigation can be summarized as follows:

1. The analytical methods used to study axisymmetric subsonic inlets at the NASA Lewis Research Center agree well with experimental results both with and without blowing BLC.

2. Blowing BLC is an effective method of controlling boundary-layer separation within a subsonic inlet.

3. For a given blowing jet total pressure ratio, an optimum slot location and height exists that minimizes the blowing jet power coefficient.

4. For the particular subsonic inlet analyzed in this study, blowing pressure ratios less than 1.5 provided the BLC momentum needed to attach the internal boundary layer.

REFERENCES

1. Chang, Paul K., Control of Flow Separation, Hemisphere, Washington, D.C., 1976.
2. Burley, R. R., and Hwang, D. P., "Experimental and Analytical Results of Tangential Blowing Applied to a Subsonic V/STOL Inlet," NASA TM-82847, 1982.
3. Johns, A. L., Williams, R. C. and Potonides, H. C., "Performance of a V/STOL Tilt Nacelle Inlet with Blowing Boundary Layer Control," AIAA Paper 79-1163, June 1979.
4. Stockman, N. O., and Farrell, C. A., Jr., "Improved Computer Programs for Calculating Potential Flow in Propulsion System Inlets," NASA TM-73728, 1977.
5. Herring, H. James, "PL2 - A Calculation Method for Two-Dimensional Boundary Layers with Crossflow and Heat Transfer," Contract Report NAS3-21810, July 1980.
6. Shaw, R. J., Williams, R. C., and Koncsek, J. L., "V/STOL Tilt Nacelle Aerodynamics and its Relation to Fan Blade Stresses," NASA TM-78899, 1978.
7. Miller, B. A., Dastoli, B. J., and Wesoky, H. L., "Effect of Entry-Lip Design on Aerodynamics and Acoustics of High-Throat Mach-Number Inlets for The Quiet, Clean, Short-Haul Experimental Engine," NASA TM X-3222, 1975.
8. Burley, R. R., "Effect of Lip and Centerbody Geometry on Aerodynamic Performance of Inlets for Tilting-Nacelle VTOL Aircraft," AIAA Paper 79-0381, Jan. 1979.
9. Abbott, J. M., "Aerodynamic Performance of Scarf Inlets," AIAA Paper 79-0380, 1979.
10. Burley, R. R., Johns, A. L., and Diedrich, J. H., "Subsonic VTOL Inlet Experimental Results," Proceedings of a Workshop on V/STOL Aircraft Aerodynamics, Naval Post Graduate School, Monterey, CA, May 16-18, 1979, Vol. II, pp. 648-664. (AD-A078909.)
11. Hwang, D. P., and Abbott, J. M., "A Summary of V/STOL Inlet Analysis Methods," Proceedings of the 13th Congress of the International Council of the Aeronautical Sciences and AIAA Aircraft Systems and Technology Conference, American Institute of Aeronautics and Astronautics, Vol. II, 1982, pp. 402-409.
12. Hess, John L., and Martin, Robert P. Jr., "Improved Solution for Potential Flow about Arbitrary Axisymmetric Bodies by the Use of a Higher-Order Surface Source Method, Part I, Theory and Results," NASA CR-134694, 1974.
13. Friedman, D. M., "Improved Solution for Potential Flow about Arbitrary Axisymmetric Bodies by the Use of a Higher-Order Surface Source Method, Part 2. User's Manual for Computer Program," MDC-J6627-02, Douglas Aircraft Co., Long Beach, CA, 1974. (NASA CR-134695.)
14. Lieblein, S., and Stockman, N. O, "Compressibility Correction for Internal Flow Solutions," Journal of Aircraft, Vol. 9, No. 4, Apr. 1972. pp 312-313.
15. Potonides, H. C., Cea, R. A., and Nelson, T. F., "Design and Experimental Studies of a Type A V/STOL Inlet," Journal of Aircraft, Vol. 16, No. 8, Aug. 1979, pp, 543-550.

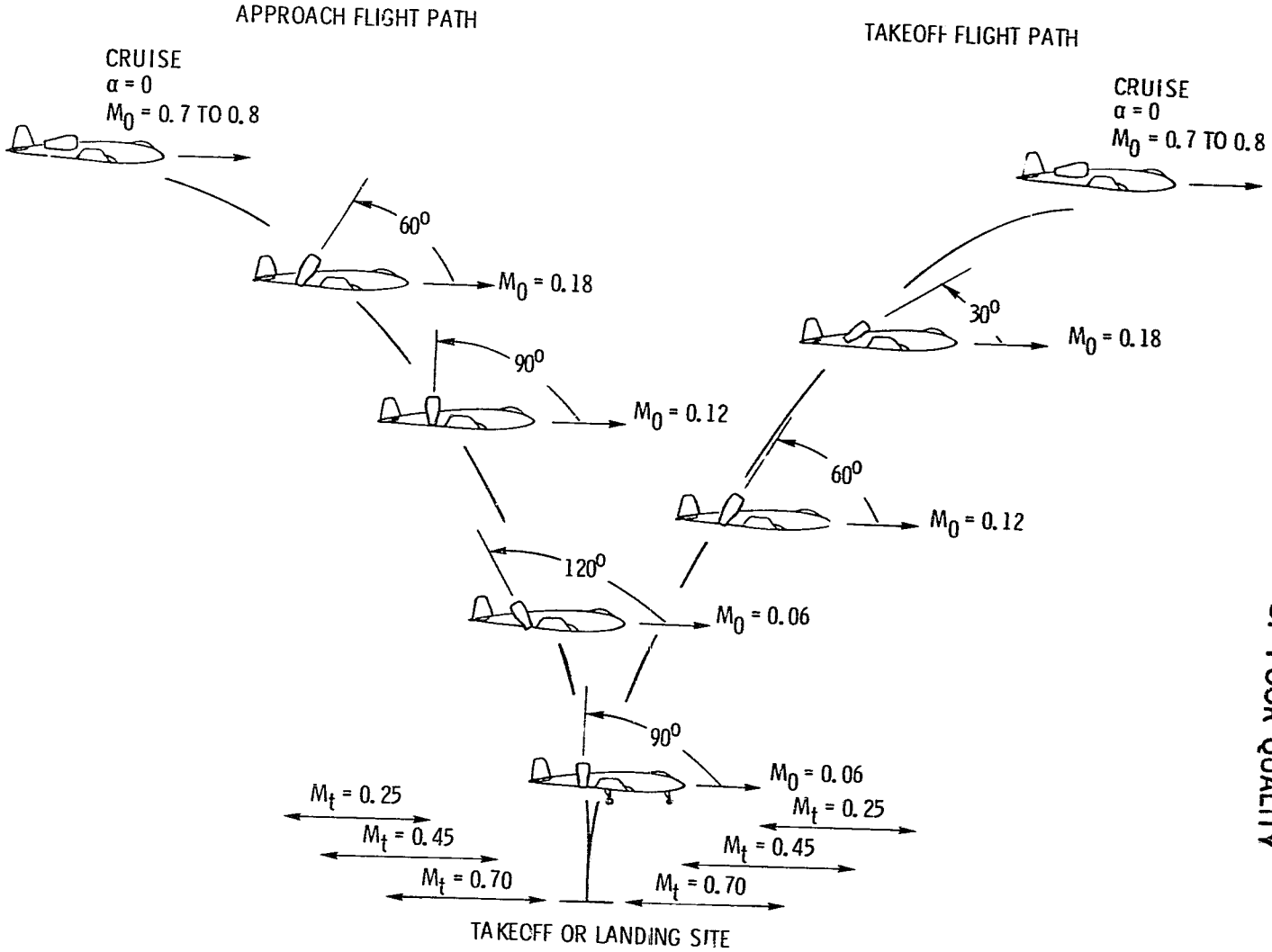

Figure 1. - Representative flight conditions for tilt-nacelle VTOL aircraft.

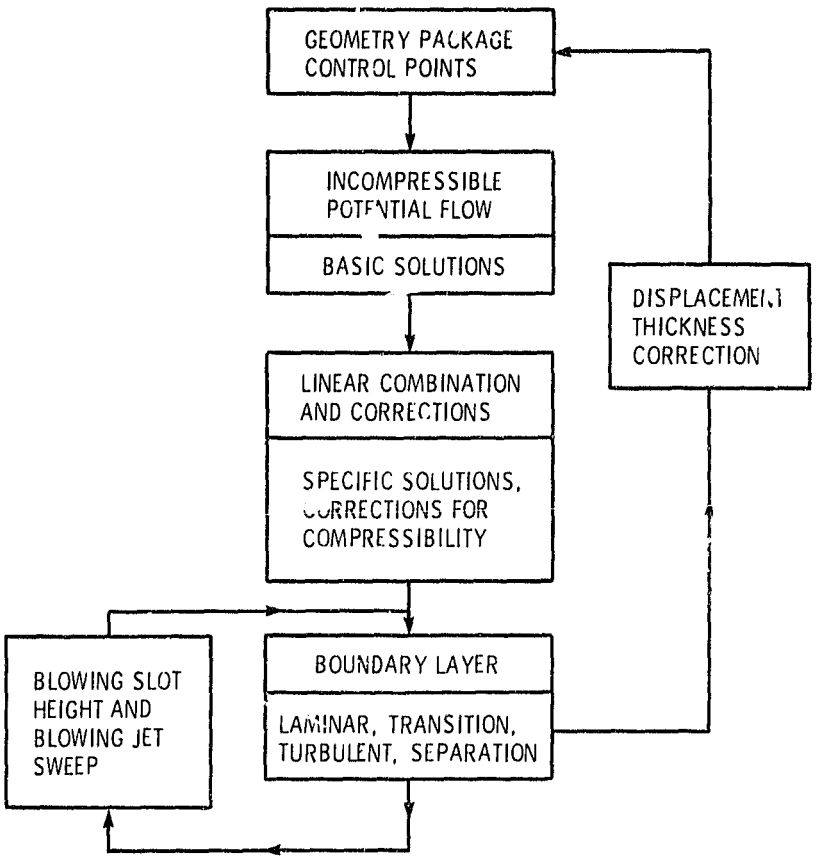

Figure 2. - Schematic diagram of method of analysis.

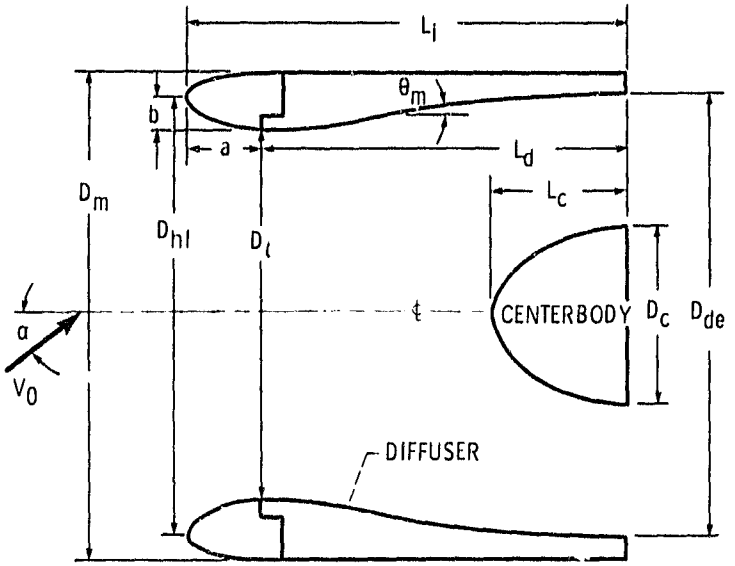

INTERNAL LIP CONTRACTION RATIO, $(D_{hl}/D_t)^2$	1.46
EXTERNAL FOREBODY DIAMETER RATIO, D_{hl}/D_m	0.905
INTERNAL LIP ELLIPSE PROPORTIONS, a/b	2.0
RATIO OF OVERALL INLET LENGTH TO DIFFUSER EXIT DIAMETER, L_i/D_{de}	1.00
RATIO OF EXIT FLOW AREA TO INLET FLOW AREA, $(D_{de}^2 - D_c^2)/D_t^2$	1.21
RATIO OF DIFFUSER LENGTH TO EXIT DIAMETER, L_d/D_{de}	0.826
RATIO OF CENTERBODY DIAMETER TO DIFFUSER EXIT DIAMETER, D_c/D_{de}	0.400
MAXIMUM LOCAL WALL ANGLE, θ_m, deg	8.7
RATIO OF CENTERBODY LENGTH TO DIFFUSER LENGTH, L_c/L_d	0.357

Figure 3. - Inlet geometry for the analytical study.

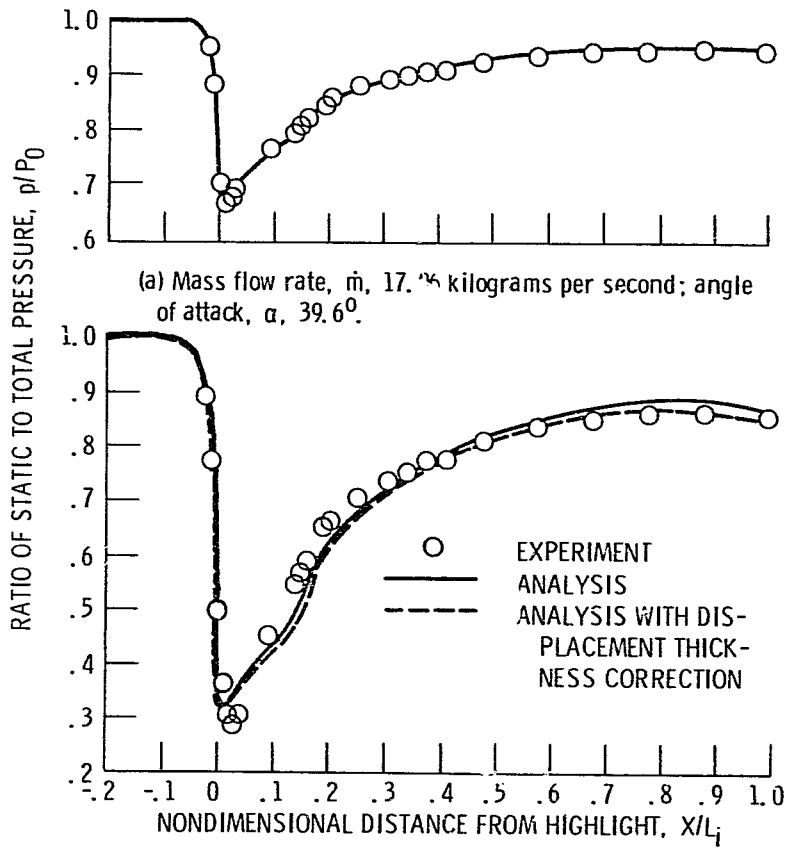

(a) Mass flow rate, $\dot{m}$, 17.[illegible] kilograms per second; angle of attack, α, 39.6°.

(b) Mass flow rate, $\dot{m}$, 27.69 kilograms per second; angle of attack, α, 44.5°.

Figure 4. - Comparison of axisymmetric potential flow calculations and experimental results. Free-stream Mach number, M_0, 0.184.

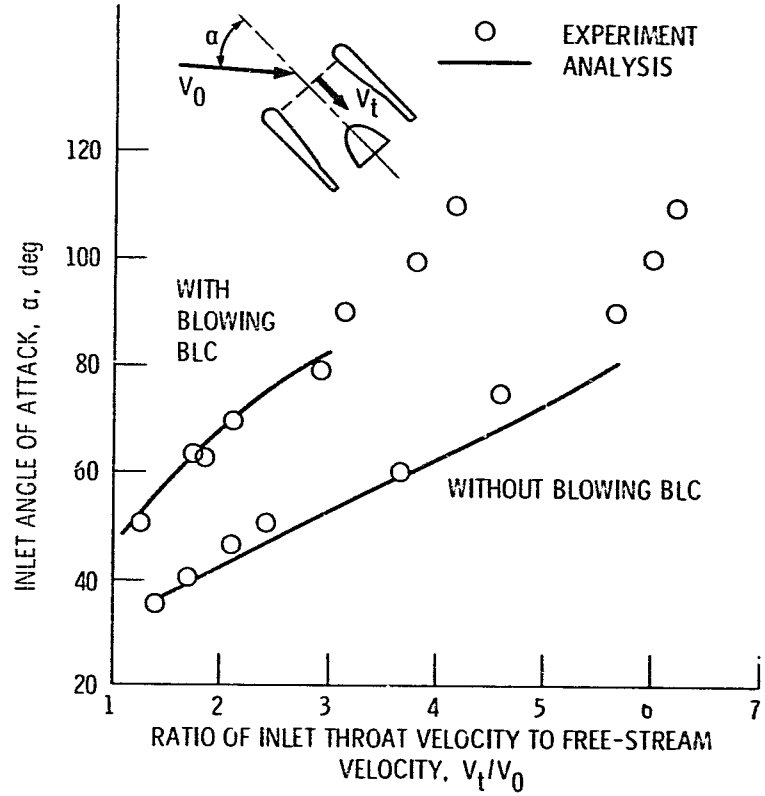

Figure 5. - Comparison of analytical and experimental flow separation boundaries with and without blowing BLC.

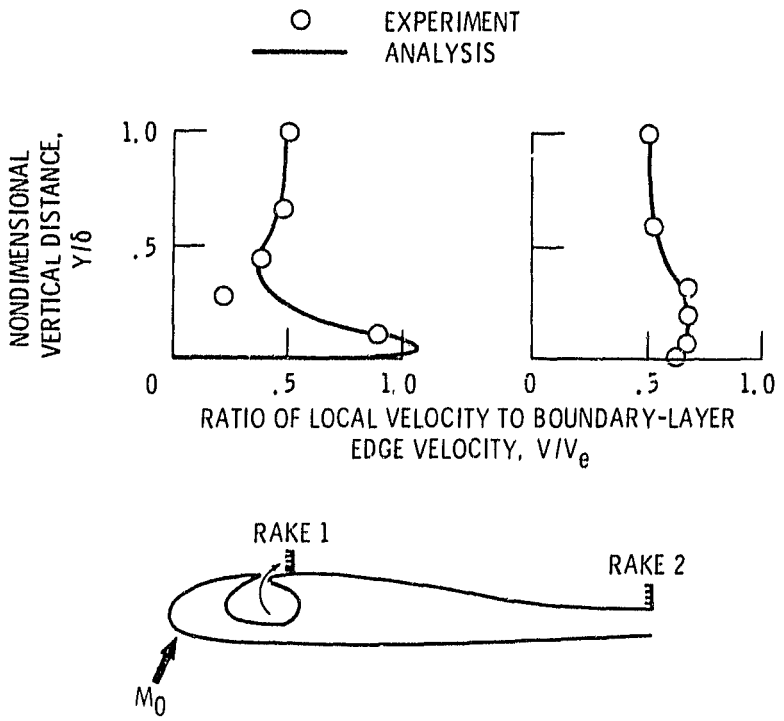

Figure 6. - Comparison of analytical and experimental velocity profiles within an inlet duct. (M_0 = 0.08; $\alpha = 70^0$; M_t = 0.168.)

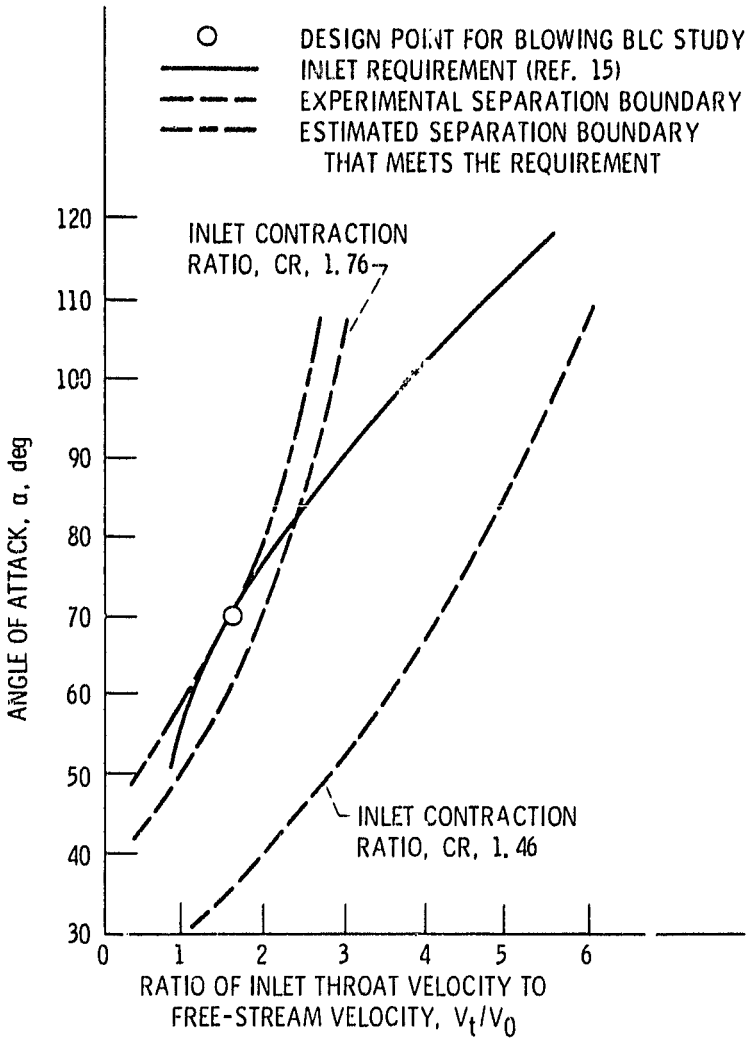

Figure 7. - Determination of inlet flow separation design point.

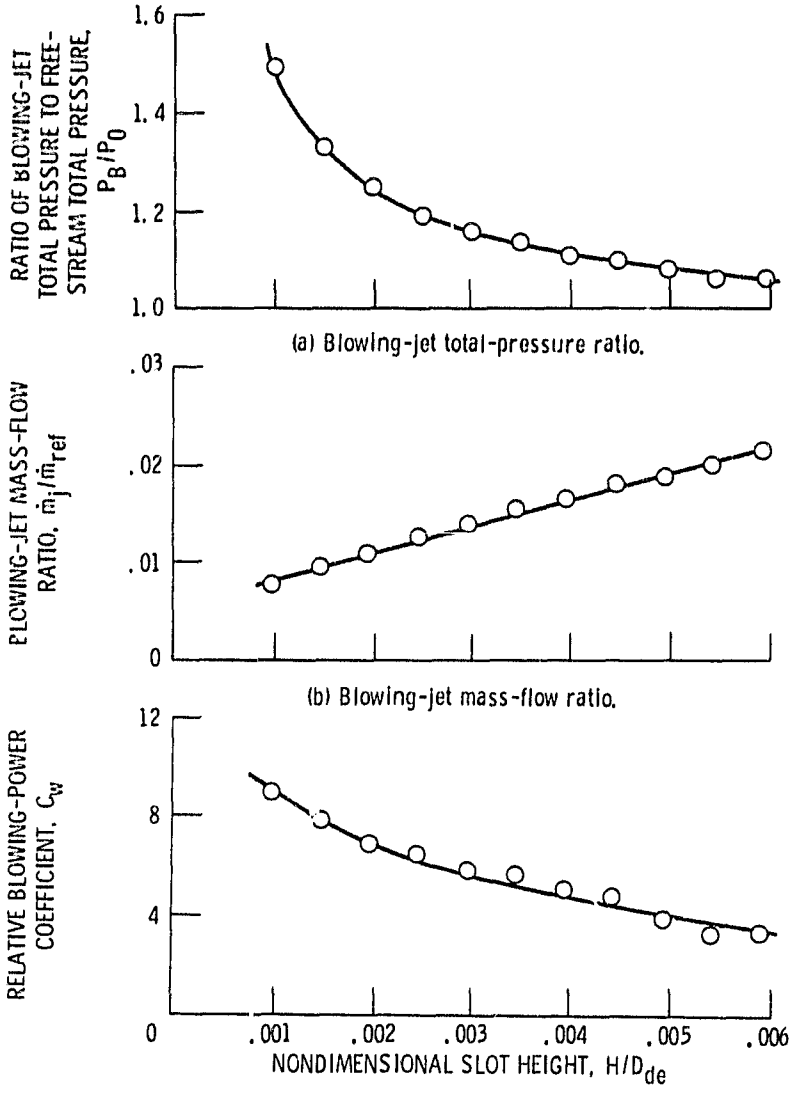

(a) Blowing-jet total-pressure ratio.

(b) Blowing-jet mass-flow ratio.

(c) Relative blowing-power coefficient.

Figure 8. - Effect of blowing slot height for a fixed location, S/L_i, of 0.55 at inlet design-point conditions (V_0 = 61 m/sec; $\dot{m}$ = 14.9 kg/sec; $\alpha = 70^0$).

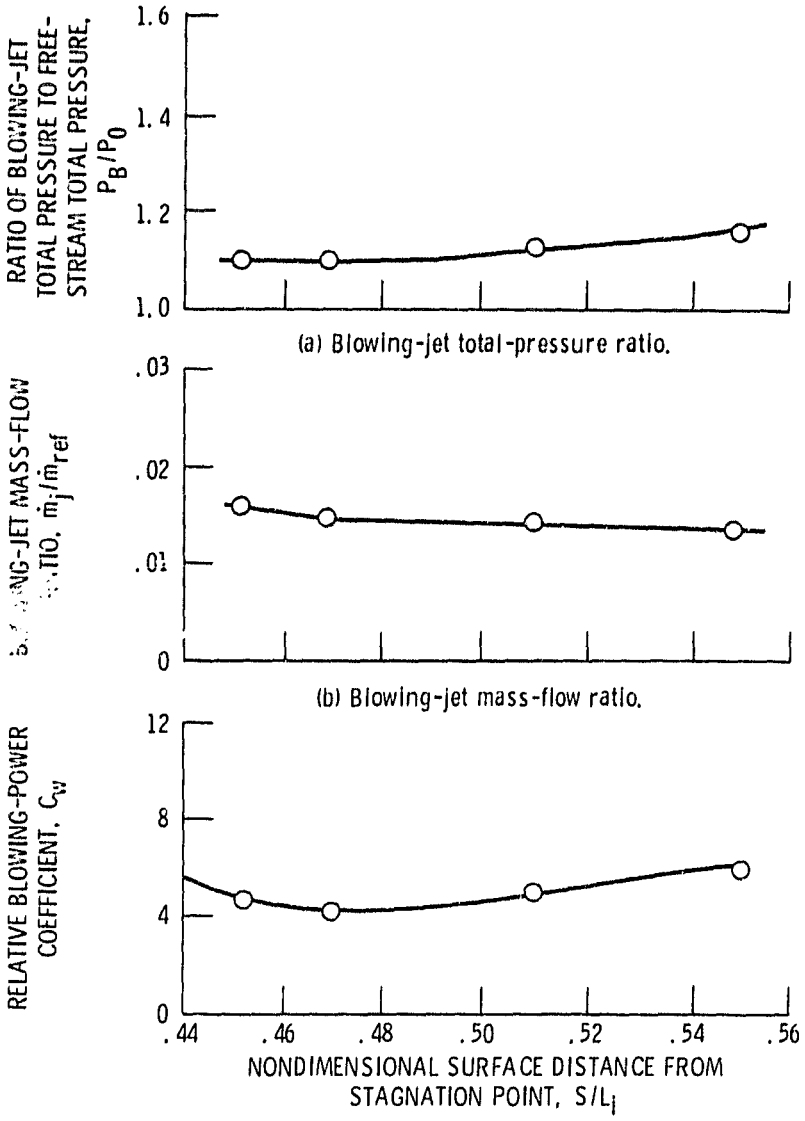

(c) Relative blowing-power coefficient.

Figure 9. - Effect of blowing-slot location for a fixed height, H/D_{de}, of 0.003 at inlet design-point conditions (V_0 = 61 m/sec; $\dot{m}$ = 14.9 kg/sec; $\alpha = 70^0$).

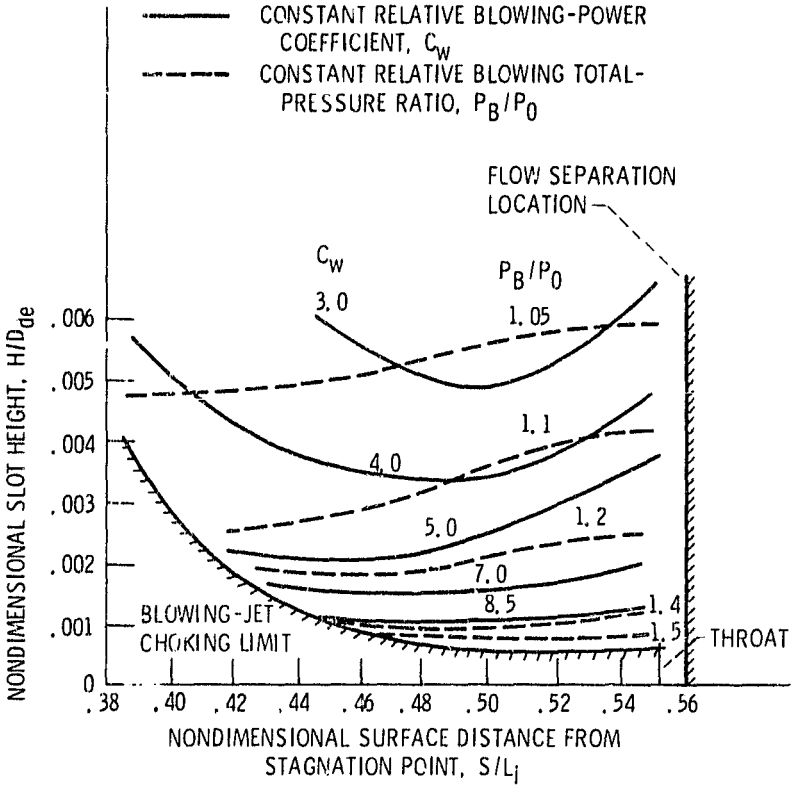

Figure 10. - Results of blowing slot optimization for inlet design described in figure 3 operating at the design point (V_0 = 61 m/sec; m = 14.9 kg/sec; $\alpha = 70^0$).